Estimation of the lattice spacing of lithium fluoride and measurement of Planck's constant using X-ray crystallography

Alie Craplet

***Abstract*—This article presents an estimation of the lattice spacing of the lithium fluoride crystal and a calculation of Planck's constant using X-ray crystallography. The distance betwen consecutive layers of the crystal was calculated as $(1.96 \pm 0.33) \times 10^{-10}$m which is in line with the theoretical value of 2.016×10^{-10}m [1]. The measured value of Planck's constant is $6.42 \pm 0.17 \times 10^{-34}$m^2.kg.s^{-1}. Again, it is a very satisfactory result regarding the accepted value of 6.626×10^{-34}m^2.kg.s^{-1} and the multiple sources of error.**

I. Introduction and Theory

SINCE its discovery in 1900, Planck's constant played a fundamental role in Physics. First proof of the quantified nature of Physics[2], Planck's constant is since 16 November 2018 used to define the base unit for mass [3]. It is therefore of paramount importance for physicists to be able to measure this constant, ideally by performing a large number of different experiments, all agreeing on the same value for Planck's constant.

A. X-Ray cristallography

X-ray crystallography is a process that involves the shooting of photons at a crystal. The word crystal is often employed in the sense of crystalline solid which is a solid whose atomic structure is highly ordered. A crystal usually consists on planes at a certain angle from one another[4]. An example of crystalline structure can be seen in Fig.1.

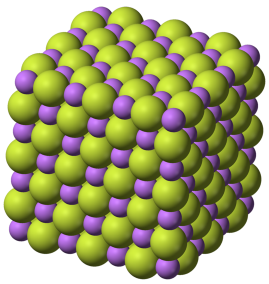

Fig. 1: Crystalline structure of lithium fluoride, the planes are evenly spaced with a separation 2.016×10^{-10}m [5][4]

When light is shined on a crystal, it can be reflected by the atoms of each layers. Depending on the plane the light is reflected on, it will travel a different distance as shown in Fig.2. This path difference causes the reflected light to experience a phase shift. As a result, the light rays reflected from different layers interfere with each other. In particular, if the path difference is an integer multiple of the wavelength of the light, the interference is constructive and a high intensity of light can be detected[]. The interference process is summarized by Bragg's law which states[6]:

$$n\lambda = \mathrm{d}\sin\theta, \tag{1}$$

where d is the spacing between consecutive planes, θ is the angle of the incident light, n is a positive integer when the interference is constructive and λ is the light's wavelength.

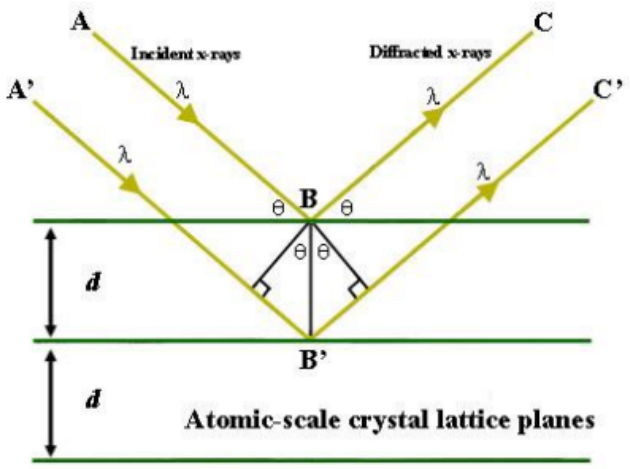

Fig. 2: Schematics for the reflection of light incoming at an angle θ by the planes of a crystal.

The typical distance between layers is of the order of the ångström [4], for example the lithium fluoride crystal has a lattice spacing of 2.016 Å[1]. Only a light with a wavelength shorter than this distance will be reflected by the atomic planes (and therefore can be used to see any reflection by the atomic planes) [4]. X-rays having wavelength between 0.01 and 10 nanometers are commonly used since they are the least energetic radiations (and therefore easiest ones to produce) sufficient to observe clear interference patterns when shined upon a standard crystal [4].

B. Production of X-rays and Bremsstrahlung radiation

X-rays are usually produced by bombarding a metal with highly energetic particles (for example electrons) inside an X-ray tube [6] as presented in Fig.3.

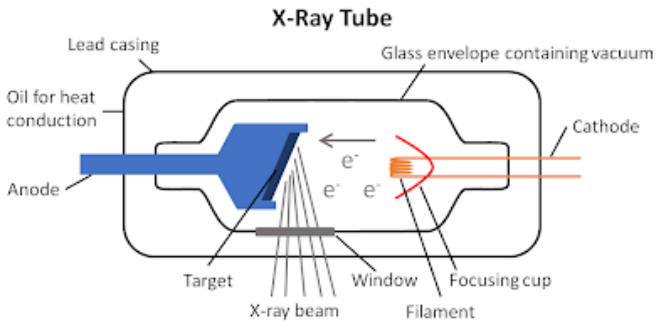

Fig. 3: Schematics of an X-ray tube. The target is often a metal (e.g. copper). The electrons are accelerated by the potential difference between the anode and cathode. This potential difference is usually between 30 and 150 keV [7].

The collision of the incident particle with a bound electron of the metal causes the expulsion of the electron from the atom and creates a vacancy in the shell it was occupying. As an electron from a higher shell falls in the available core hole, a photon of a specific wavelength is emitted. When the electron holes are produced in the K shell, the wavelength of the photon resulting in the jump of an electron from the L shell to the K shell is denoted as K_α and the photon due to the fall of an electron from the M shell to the K shell is referred to as K_β. The wavelength of these emissions is often in the X-ray part of the light spectrum and they are called the atom's characteristic X-rays[8]. When using a copper atom as target, the K_α photons are more likely to be produced than the K_β ones. Their energies are respectively 8037 ∓ 2eV and 8037 ∓ 2eV and 8904 ∓ 2eV[6]

When charged particles such as electrons are fired at atoms, they can also come close to the nucleus and get deviated by this highly charged object [9].

Due to the electromagnetic force and their light mass compared to the nuclei, the electrons get deflected from their initial trajectory [10]. They must therefore decelerate[11] and hence lose energy in the form of radiations [10]. These radiations are called bremsstrahlung radiations from the german "braking radiations". Since this process is random by nature the energy associated with each deceleration varies for each case. This gives rise to a continuous spectrum of bremsstrahlung radiations. An example is shown in Fig.4.

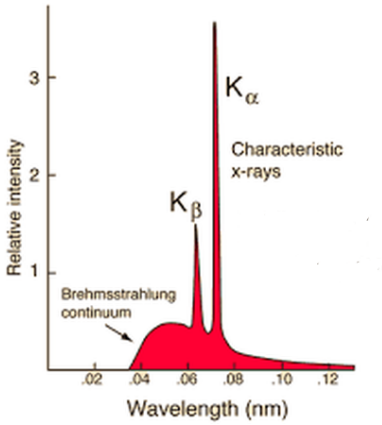

Fig. 4: Characteristic profile of the spectrum of the wavelength of the photon produced by an X-ray tube. The two sharp peaks correspond to the characteristic X-rays of the material. The continuum is due to bremsstrahlung radiations and has a higher intensity for more energetic photons[8]. For small wavelenghts, the continuum has a linear trend.

If the electron is brought to a complete stop by its interaction with the nuclei, then all its kinetic energy is transferred to the emitted photon giving a bremsstrahlung of maximal energy and minimal wavelength λ_{max} [10]. For an electron whose kinetic energy comes from being accelerated inside an electrical potential V the value of the minimal wavelength is given by the Duane-Hunt law [12] as,

$$\lambda_{max} = \frac{hc}{eV}, \tag{2}$$

where h is Planck's constant, e is the elementary unit of charge and c is the speed of light.

By considering the deflection from the electron's initial path as a function of the atomic charge of the nuclei, professor Hans Kramers found the following expression for the bremsstrahlung spectrum[10]:

$$I(\lambda) = \frac{K}{\lambda^2}\left(\frac{\lambda}{\lambda_{max}} - 1\right), \tag{3}$$

where $I(\lambda)$ is the intensity of the radiation of wavelenght λ, K is a constant proportional to the atomic number of the target.

II. Experimental Method

This study used Tel-X-ometer linked to a Geiger counter as well as a set of crystals. The Tel-X-Ometer is composed of an fixed X-ray canon, a rotating asupport and a crystal platforms. The Geiger-Müller tube of a Geiger counter was mounted on the rotating plateform. The electric potential inside the X-ray canon was 30keV. A lithium fluoride crystal was placed on the path of the photons and the intensity of the detected light was recorded as a function of the angular position of the counter. A picture of the Tel-X-Ometer can be seen in Fig 5.

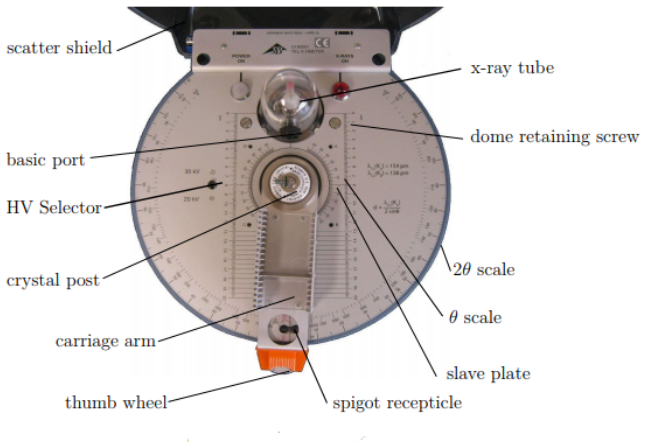

Fig. 5: Picture of a Tel-X-Ometer similar to the one used in this experiment.The thumb wheel is graduated in $1/6^{\text{th}}$of a degree. For this experiment, a Geiger-Müller tube was fixed to the rotating carriage arm [8].

To improve accuracy the crystal was carefully cleaned with absorbent paper before each set of measurements. Gloves were worn whenever the crystal was touched to preserve its fragile surface. A comparison of the intensity of the radiation peaks with respect to the orientation of the crystal was also realized in order to choose the orientation of the crystal giving the clearer signal.

This study was realized in two steps. First, the intensity of detections was recorded over the full range of angles ($10°$ to $120°$) in $1°$ increments. These values correspond to a measurement of twice the scattering angle θ (see section I). This step aimed at highlighting the presence of Braggs peak and observing the bremsstrahlung continuum (see section I). This first step acted therefore as a preliminary verification of the suitability of lithium fluoride for the determination of Planck's constant.

Then, precise measurements were done each $1/12^{\text{th}}$ of a degree over the range of $11°$ to $24°$. The lower limit was set by the appartus whose structure does not allow measurments below $11°$.

As explained in section I, the aim of this measurement was to realize a fitted plot of the Bremsstrahlung continuum. It was therefore decided to take a maximum amount of data points rather than repeating the same few measurements multiple times.

III. Results

A. Sources of error

The sources of error involved in this experiment are summarized in Table I. The main sources of error and the calculation of their magnitude are discussed in this section.

The initial misalignment was measured before measurements were taken by rotating the x-ray canon and checking the value of the $0°$ and $45°$ on the θ and 2θ scales. The Vernier scale used was graduated in $\frac{1}{6}^{\text{th}}$ of a degree and measurement were realized every $\frac{1}{12}^{\text{th}}$ of a degree. The error on the angle was therefore estimated as more than one half of $\frac{1}{12}^{\text{th}}$ of a degree. A measurement of the angles considered as corresponding to the same angular value was also realized giving an spread of $\frac{1}{20}^{\text{th}}$ of a degree.

The system's dead time affect was considered as negligible since it was showed that at specific angles radiation rates much bigger (more than 1000 times higher) than the one measured when estimation Planck's constant were still well recorded (see section III.B.).

The systematical error due to the crystal's imperfections was not calculated due to lack of time. The method used for this estimation would have been to compare the results with different positions of the crystal to find the standard deviation in measurements. However, this process would be very long and the error due to crystal is thought as being small compared with the other sources of error.

It was also noticed that the Geiger counts started at 1 counts and not 0, both when the X-ray beam was on and when it was not. This systematical error was accounted for by subtracting one count to each measurement.

TABLE I: Summary of the sources of error and their relative magnitude as well as methods used to reduce them

Source of error	Magnitude	Methods for reducing the relative impact
Initial misalignment	$\pm 0.1°$	Reclamping the knurled ring[]
Parallax effect	$\pm\frac{1}{20}°$	Use a Vernier scale with smaller radiations. For consistency, the same experimentalist should do all the measurements
Radiation count starting at 1	$+1$ count for each measurement	Subtract 1 count to the data. Take longer measurements (e.g. 30s) to reduce relative error
Cleanness of crystal and potential scratches on the surface	To be determined by further investigations	Carefully clean the crystal before each set of measurements. Repeat measurements with different LiF crystals and/or X-ray beam centered on different region of the same crystal
Background radiations (electric noise in the cables, ambient radioactivity...)	Negligible[13]	Do experiment in an otherwise empty laboratory. Shield the Tel-X-Ometer with radiation absorbant material (e.g. lead)
System's dead time	Negligible	Make measurements with controlled emission rate to determine the precise dead time of this system

All the non-negligible errors except the parallax effect are systematical errors. The error on each measurement of the

angle corresponds to the sum of magnitude of each source of error. Its value is $\pm 0.15°$.

B. Calculation of the lattice spacing for the lithium fluoride crystal

The number of counts as a function of the scattering angle is summarized in Fig 6. Peaks corresponding to the Bragg's interference of order n=1 and n=2 (see section I) should be noted.

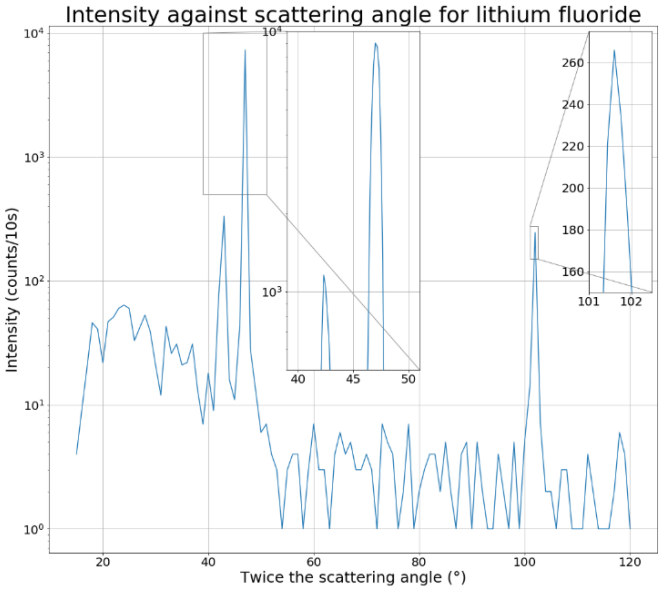

Fig. 6: Plot of the intensity of counts as a function of twice the scattering angle. The three clear peaks have a scattering angle of $21.17°$, $23.5°$ and $50.83°$. They correspond respectively to the Bragg peaks of degree n=1 for the K_β and K_α and of degree n=2 for the K_α radiation. The second peak corresponding to the K_β radiation is located at $43.33°$ but has an intensity too low to be clear on this plot.

From Fig 6. and eq(1), the distance between the layers of the lithium fluoride crystal can be calculated as being $(1.96 \pm 0.34) \times 10^{-10}$m. The statistical error has a value $\pm 0.18 \times 10^{-10}$ which is less than the true value of the error as determined in section III.A. This experimentally determined value is close to the accepted value of 2.016×10^{-10}m [1].

C. Measurement of Planck's constant

The data collected data over the small angles can be seen in Fig 7. As explained in section I, the aim of this study was to compute the angle at which the detection of the photons with the highest energy is made. This angle θ_{min} is the value of the angle of the intercept of the signal with the x-axis.

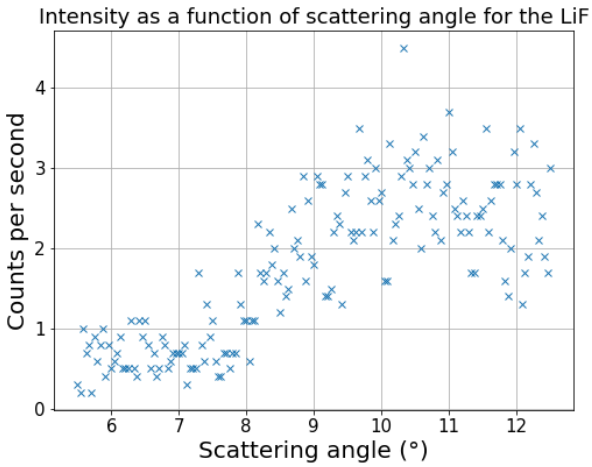

Fig. 7: Intensity of detection for small angles. The background is represented by the horizontal line before $7.5°$ and of value between 0.1 and 1.1 counts per second. The specific profile can be pictured from this data. The high level of fluctuations should be mentioned.

As noted in Fig 4 the expected continuum as as linear trend close to its minimum value. A first fitting of the data was therefore realized using a linear function. To choose which portion of the curve had to be linearly fitted, the following assumption was made: 'the linear region is symmetrical about a middle point'. This assumption allowed a quantitative determination of the best linear fit. Its validity is discussed later in this section.

The goodness of fit was calculated using the Python function scipy.stats.linregress. The middle point of the linear region as well as the total number of points in the linear region were varied. Fig 8 summarizes the goodness of the best linear fit as a function of the chosen middle point. It should be noted that the best fits have a middle point between $8.5°$ and $8.75°$ with an absolute maximum for the goodness of fit occurring at the angle $8.71°$.

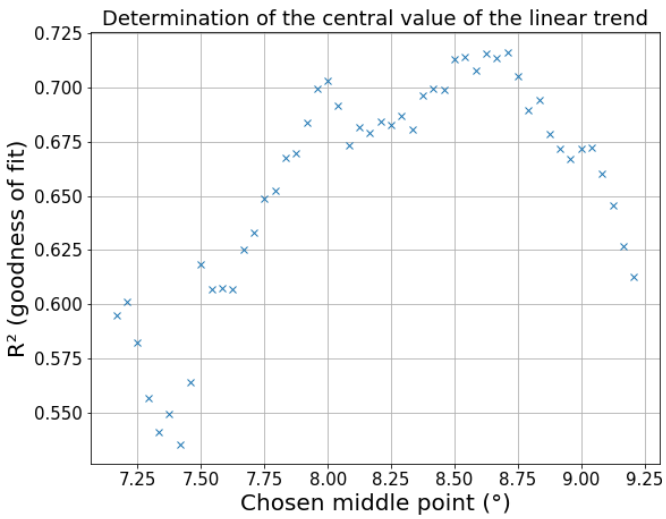

Fig. 8: Comparison of the goodness of the best line of fit achievable depending on the center of the linear region.

Then, the length of the region to be plotted was determined by calculating the goodness of the fits with middle point $8.71°$ and varying number of points on each side of this middle points. Results are shown in Fig. 9.

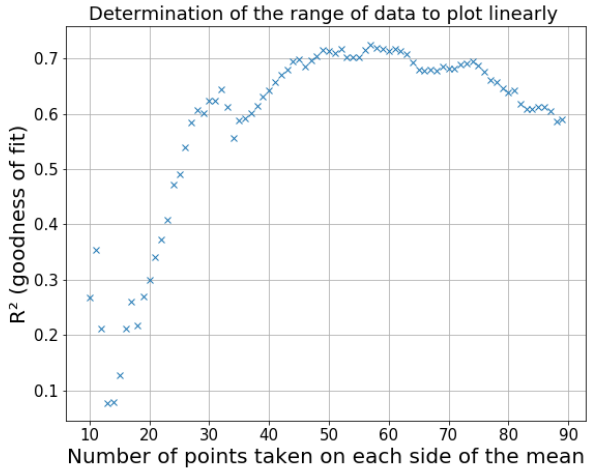

Fig. 9: Comparison of the goodness of fit as a function of the number of points taken on each side of $8.71°$. From this graph, the best interval has 57 points on each side of the mean.

From Fig.9, the best linear fit is therefore centered on $8.71°$ and spans between $12.08°$ and $21.58°$. This fit and its equation can be seen in Fig. 9. This scattering angle is converted into a photon's wavelength using eq(1). The intercept of the fit with the x-axis is $\theta_{min} = 5.71° \pm 0.15°$ where the error has the value estimated in section III.A. The statistical error has a smaller value of $0.11°$. This corresponds to a wavelength $\lambda_{min} = (2.01 \pm 0.05) \times 10^{-11}$. Using this value of λ_{min}, the value of the lithium fluoride lattice spacing given in section I, the value of the electric potential trough which electrons were accelerated and eq(2), the value of $h_{lin} = (6.42 \pm 0.17) \times 10^{-34}\text{m}^2.\text{kg.s}^{-1}$ was obtained for Planck's constant.

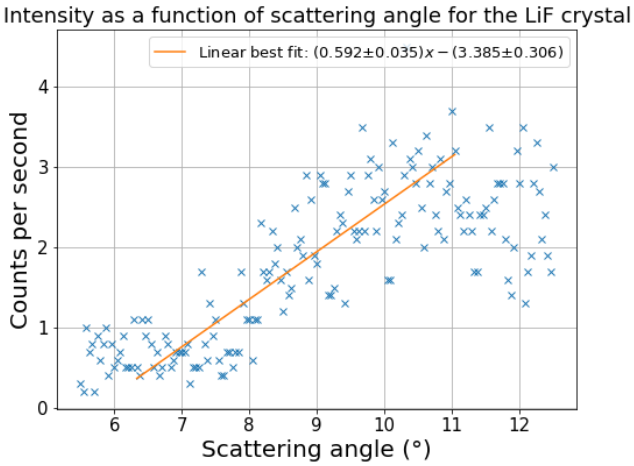

Fig. 10: Intensity of detection for small angles fitted linearly over the optimal range of points.

However, this method is an approximation and fitting the set of points using Kramer's rule (see section I.B.) should be more accurate. The same data set was fitted using Kramers law (see eq(3)). The result is pictured in Fig 10 where the wavelength of the photons is calculated from the value of the scattering angle using eq(1). Only wavelength from 0.05nm had a count higher than the background level. Only these points were therefore fitted.

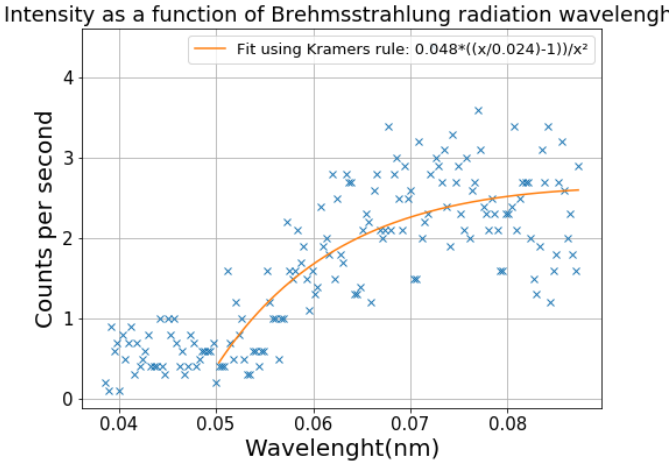

Fig. 11: Intensity of detection for small wavelengths, corresponding to high energy photons and small scattering angles fitted using Kramers law. the shift in the count was accounted for.

From Fig.10 the intercept of the curve of best fit with the x-axis is $\lambda_{min} = (2.43 \pm 3.06) \times 10^{-12}\text{m}$ which gives an estimation for Planck's constant of

$h_{Kram} = (7.77 \pm 9.79) \times 10^{-34}\text{m}^2.\text{kg.s}^{-1}$ using eq.(2) and the statistical error calculated on Pyhton. The statistical error is hosen upon the experimentally estimated value because it has a higher value.

This value is further away from the accepted value of h $= 6.626 \times 10^{-34}\text{m}^2.\text{kg.s}^{-1}$than h_{lin}, however this argument is not sufficient to say that the value of h_{lin} should be used over the value h_{lin}. A method for estimating which fit is more accurate is to calculate the average square of the residual for each fit using the following equation[14]:

$$S = \frac{\sum_i (y_i - f(x_i))^2}{N}, \tag{4}$$

where y_i are the data points,$f(x_i)$ are the corresponding value of the fit and N is the number of points considered in the fit. The S values of the linear fit and the fit using Karmers law are respectively $S_{lin} = 0.25$ and $S_{Kram} = 0.33$. The linear fit is therefore more accurate and should be used over the Kramers fit to calculate the intercept of the data points with the x-axis.

A possible explanation for the relatively low precision of the Kramers fit is the lack of data corresponding to angles higher than $24°$. Had more data points been taken, it would have been possible to fit the data using Kramers rule better.

IV. Conclusion

This paper presents the utilization of X-ray crystallography to determine a crystal's layer spacing and estimating Planck's constant from the specific aspect of the bremsstrahlung continuum. The layer spacing of the lithium fluoride was calculated as $(1.96 \pm 0.33) \times 10^{-10}$m. This value agrees well with the accepted value of 2.016×10^{-10} [1] which is contained within its margin of error.

The X-ray continuum was fitted to two different functions. The linear fit proved to be more accurate than the one realized using Kramers law (see section III. C) because of the range of angles over which the measurements were realized. Planck's constant was therefore calculated as being $6.42 \pm 0.17 \times 10^{-34}\text{m}^2.\text{kg.s}^{-1}$. This setup allowed a great level of precision and the experimental value differs from the theoretical value of $6.626 \times 10^{-34}\text{m}^2.\text{kg.s}^{-1}$ by only 3.0%.

The main sources of error in this experiment were the systematical error of the radiation count starting at 1 count and the random error in the estimation of the scattering angle (mostly due to parallax effect and consistency issues).

Overall, this experiment was very successful at presenting the basis of crystallography and the phenomenon of bremsstrahlung radiation. Its relatively low level of error and its ease of use make of this experiment an efficient way to measure Planck's constant. This experiment could be improved by taking a wider range of data over the small angles region as well as counting detections for a longer time than 10 seconds hence reducing the fluctuations in the data and potentially leading to a fit using Kramers rule more precise than the linear approximation.

Acknowledgment

The author would like to thank her lab partner and the lab demonstrators for their invaluable help and advices.

References

[1] National Center for Biotechnology Information, "Pubchem compound database." [Online]. Available: https://pubchem.ncbi.nlm.nih.gov/compound/224478 (accessed Dec 2, 2018)
[2] M. F. L'Annunziata, *Radioactivity : introduction and history*. Oxford: Elsevier, 2007.
[3] P. Richard, H. Fang, and R. Davis, "Foundation for the redefinition of the kilogram," *Metrologia*, vol. 53, no. 5, p. A6, 2016. [Online]. Available: http://stacks.iop.org/0026-1394/53/i=5/a=A6
[4] J. S. Blakemore, *Solid state physics*, 2nd ed. Cambridge: Cambridge University Press, 1985.
[5] Wikimedia Commons. [Online]. Available: https://en.wikipedia.org/wiki/File:Lithium-fluoride-3D-ionic.pngfilelinks
[6] The Imperial Physics Second Year Laboratory, "Solid state physics experiment," 2018.
[7] [Online]. Available: https://sites.google.com/site/frcrphysicsnotes/production-of-x-rays
[8] Georgia State University, "Hyper physics." [Online]. Available: http://hyperphysics.phy-astr.gsu.edu/hbase/quantum/xrayc.html
[9] H. A. Kramers, *Die Grundlagen der Quantentheorie : Quantentheorie des Elektrons und der Strahlung*, ser. Hand- und Jahrbuch der chemischen Physik ; Bd. 1. Leipzig: Akademische Verlagsgesellschaft, 1938.
[10] ——, "Xciii. on the theory of x-ray absorption and of the continuous x-ray spectrum," *The London, Edinburgh, and Dublin Philosophical Magazine and Journal of Science*, vol. 46, no. 275, pp. 836–871, 1923.
[11] T. Horbury, "Lectures on classical mechanics," 2017.
[12] Anonymous, "On x-ray wave-lengths," *Physical Review*, vol. 6, no. 2, pp. 166–172, 1915.
[13] G. F. Knoll, *Radiation, detection and measurement*, 3rd ed. New York ; Chichester: Wiley, 2000.
[14] M. Richards, "Lectures on statistics," 2018.